Morphopoietic Determinants of HIV-1 Gag Particles Assembled in Baculovirus-Infected Cells

Bernard Gay, Jeannette Tournier, Nathalie Chazal, Christian Carrière, Pierre Boulanger

VIROLOGY 247, 160–169 (1998)
ARTICLE NO. VY989237

Morphopoietic Determinants of HIV-1 Gag Particles Assembled in Baculovirus-Infected Cells

Bernard Gay, Jeannette Tournier, Nathalie Chazal, Christian Carrière, and Pierre Boulanger[1]

Laboratoire de Virologie et Pathogénèse Moléculaire (CNRS UMR 5812), Faculté de Médecine, 34060 Montpellier, France

Received January 7, 1998; returned to author for revision March 24, 1998; accepted May 12, 1998

The determinants for HIV-1 particle morphology were investigated using various deletion and insertion mutants of the Gag precursor protein (Gag) expressed in baculovirus-infected cells and ultrastructural analysis of membrane-enveloped Gag particles under the electron microscope. Five discrete regions were found to influence the size, the variability in dimension, and the sphericity of the particles: (i) the matrix (MA) N-terminal domain, within residues 10–21, the junctions of (ii) MA–CA (capsid), (iii) CA-spacer peptide SP1 and (iv) nucleocapsid (NC)–SP2, and (v) the $p6^{gag}$ C-terminus. Internal regions (ii), (iii), and (iv) contained HIV-1 protease cleavage sites separating major structural domains. No particle assembly was observed for *amb*276, a MA–CA polyprotein mutant lacking the C-terminal third of the CA domain. However, MA–CA domains including the MHR (residues 277–306), or downstream sequence to CA residue 357, resulted in the assembly into tubular or filamentous structures, suggesting a helical symmetry of Gag packing. Mutant *amb*374, derived from *amb*357 by further addition of the heptadecapeptide motif ^{358}HKARVLAEAMSQVTNSA^{374}, overlapping the CA–SP1 junction and the SP1 domain, showed a drastic change in the pattern of Gag assembly, compared to *amb*357, with formation of spherical particles. These data suggested a novel function for the spacer domain SP1, acting as a spherical shape determinant of the Gag particle which would negatively affect the helical symmetry of assembly of the Gag precursor molecules conferred by the MHR and the downsteam CA sequence, within residues 307–357.

Key Words: HIV-1; Gag precursor; assembly; morphological determinants; p6; SP1; SP2 domains; MA–CA junctions; helical symmetry; MV and CDV nucleoprotein core.

INTRODUCTION

The occurrence of virus-like particles in cells expressing solely the human immunodeficiency virus type 1 (HIV-1) Gag precursor (Pr55Gag) implied that this polyprotein contained all the sequence information required for its self-assembly into immature Gag particles, which, upon maturation, lead to infectious virions (Wills and Craven, 1991; Craven and Parent, 1996). Extensive mutagenesis of the retrovirus Gag structural domains, matrix (MA), capsid (CA), nucleocapsid (NC), and C-terminal p6 (reviewed in Boulanger and Jones, 1996; Craven and Parent, 1996; Kräusslich and Welker, 1996), and crystallographic analysis of MA (Hill *et al.,* 1996; Massiah *et al.,* 1994; Rao *et al.,* 1995) and CA proteins (Gamble *et al.,* 1996, 1997; Gitty *et al.,* 1996; Kovari *et al.,* 1997; Momany *et al.,* 1996) have contributed to defining the regions in the Gag precursor which are essential for interaction and self-assembly of membrane-enveloped, budding particles. In RSV, three discrete assembly domains have been identified, and termed M, for membrane-binding, I, for interaction, and L, for late step of budding (Craven and Parent, 1996). In HIV-1 Pr55Gag, M has been found to be confined to the N-myristoylated glycine and the N-terminal 31 residues of the MA domain, I has been mapped to the NC domain, and L at the N-terminal end of the p6 domain (Craven and Parent, 1996).

Virus particle morphogenesis has to be considered from a double point of view: (i) the quantitative aspect of the phenomenon, which can be assayed by the number of particles recovered from the extracellular medium, and its decrease or absence in the case of assembly-defective mutants; (ii) the qualitative analysis of the assembly process, which takes into account the parameters of the particles, i.e., their mean size, shape, and regular or irregular contours. In the case of HIV-1, however, the effects of *gag* mutations on particle assembly have mainly been studied in quantitative terms, and the numbers of Gag particles and mature infectious virions produced have been evaluated by CA immunoassays and RT enzymatic assays. By contrast, very little has been reported on the regions of the Gag precursor molecule and on the mechanisms which control the size, the shape, and the symmetry of the particles.

The present study describes the results of an ultrastructural analysis performed by electron microscopy (EM) on membrane-enveloped Gag particles assembled and released by baculovirus-infected insect cells expressing recombinant HIV-1 Gag precursor mutants. This system has the advantage of a high efficiency of Gag

[1] To whom reprint requests should be addressed at Laboratoire de Virologie & Pathogénèse Moléculaire, Faculté de Médecine, 2, Boulevard Henri IV, 34060 Montpellier Cedex, France. Fax: 33 (0)4 67 54 23 78. E-mail: pboulang@infobiogen.fr.

0042-6822/98 $25.00

precursor production and particle assembly (Boulanger and Jones, 1996; Carrière *et al.,* 1995; Chazal *et al.,* 1994, 1995; Gheysen *et al.,* 1989; Hughes *et al.,* 1993; Luo *et al.,* 1994; Overton *et al.,* 1989; Royer *et al.,* 1991, 1992); and provides Gag particle samples in sufficient amounts to obtain statistical data with reasonable confidence.

RESULTS

Electron micrographs showing WT and mutant Gag particles at the periphery of sectioned cells were observed and the parameters of the particles determined (Fig. 1 and Table 1). It was assumed that they represented nascent or "young" particles freshly released by budding from the plasma membrane. The results, exemplified in Figs. 3 and 4, are summarized in histograms of Figs. 2a, 2b, and 2c. Figure 2a presents the mean values for the external diameter of the mutant Gag particles. Their heterogeneity in size was estimated by the standard deviation (SD) of the mean values (Fig. 2b). Their propensity to assemble into nonspherical particles was estimated from the mean ratio of the minimum diameter (*d*) to the maximum diameter (*D*), defined as the sphericity index (*d:D*) (Fig. 2c and Table 2).

With the exception of mutant *amb*276, all the other mutants released extracellular Gag particles in significant numbers. The diameter of Sf9-released WT Gag particles was found to be 125.04 $\pm$ 12.45 nm (mean $\pm$ SD; $n = 51$; confidence interval = 3.5 nm at the $P = 0.05$ level), consistent with the previously reported dimensions of mature and immature HIV-1 particles (135–150 nm in diameter) observed by conventional transmission EM (Gelderblom, 1990). However, our recombinant WT Gag particles appeared to be rather homogeneous in size, a result which contrasted with the wide range of diameters, varying from 120 to 260 nm, for similar recombinant Gag particles analyzed by cryo-EM (Fuller *et al.,* 1997). It is not possible to assess whether the homogeneity in size and shape of the WT Gag particles resulted from the artifactual effect of fixative and contrasting agents used in our EM study or, alternatively, whether the nascent, fibrin-included particles found in the vicinity of Sf9 cell plasma membrane would have been preserved in their original, native morphology. In the latter case, this would imply that heterogeous Gag particles harvested from the culture medium and isolated by ultracentrifugation in velocity gradients for cryoEM analysis (Fuller *et al.,* 1997), could have undergone some morphological alterations.

In contrast to WT Gag particles, more pleiomorphism was shown by Gag mutants, although to various degrees (Figs. 2–4). At the N-terminal extremity of the Gag precursor molecule, in the MA domain, the deletion *dl*10-21 (refer to Figs. 5c and 5d in Chazal *et al.,* 1995), corresponding to the first α-helix H1, and the deletion *dl*101-143 (Fig. 3b), corresponding to the last α-helix H5 (Hill *et al.,* 1996; Massiah *et al.,* 1994) and the MA–CA junction, resulted in mutant particles significantly larger than the WT particles, with diameters of 206.01 $\pm$ 64.70 and 187.90 $\pm$ 37.13 nm, respectively (Fig. 2a). The *dl*41-143 mutant (Fig. 3a) had a diameter of 165.82 $\pm$ 26.90 nm, intermediate between the WT particles and the *dl*10-21 and *dl*101-143 mutant particles. The *dl*10-21 mutant particles and, to a lesser degree, the *dl*41-143 and *dl*101-143 showed a higher heterogeneity in size and shape than the WT Gag particles, with a significant number of nonspherical particles adopting a dumbell shape (Figs. 2b, 2c, 3a, and 3b).

At the other extremity of the Gag precursor molecule, the deletion of the C-terminal half of $p6^{gag}$, as in *amb*462, the deletion of the entire $p6^{gag}$ domain and most of the SP2 intermediate domain, as in *amb*438, or the deletion of $p6^{gag}$, SP2, and the C-terminal end of the NC domain, as in *amb*426, had little or no effect on the final sizes of the mutant particles: 132.86 $\pm$ 9.19, 120.43 $\pm$ 10.02, and 127.04 $\pm$ 11.13 nm, respectively (Fig. 2a). Likewise, partial or total deletion of the $p6^{gag}$ domain seemed to result only in minor changes in the degree of homogeneity and sphericity of mutant particles: a standard deviation of the mean value slightly lower than that for WT was observed for *amb*462 (9 nm vs 12 nm for WT; Fig. 2b) and a slightly higher sphericity index for *amb*438 (0.93 $\pm$ 0.06 vs 0.89 $\pm$ 0.01 for WT; Fig. 2c and Table 2). In contrast to these deletions, the fusion of an extra retroviral sequence to the carboxy-terminal extremity of $p6^{gag}$, as in GagPR67, apparently affected the particle size and homogeneity to a greater extent. GagPR67, which contains a $p6^{gag}$-fused protease (PR) domain inactivated by a D33G mutation at its active site, released irregular particles, varying in shape from small spherical particles to elongated structures (Royer *et al.,* 1997). Their mean diameter was found to be slightly smaller than that of WT particles ($m = 109$ nm; Fig. 2a), but their heterogeneity (SD = 77.32 nm) and lack of sphericity ($d:D = 0.79$) were both higher (Figs. 2b and 2c). Further addition of portions of the reverse transcriptase domain (Pol) at the C-terminus of Gag polyprotein, as in GagPRPol84 or GagPRPol112 constructs (Royer *et al.,* 1997), abolished assembly and budding (not shown).

Since the quantitative changes occurring with p6 mutations were rather discrete, in comparison to carboxy-truncated mutants such *amb*333 or *amb*341, the Student's test was applied to the parameters of the WT, *amb*462, *amb*438, and GagPR67 particle populations. The difference in particle heterogeneity was apparently significant at the $P = 0.05$ level between WT and *amb*462 ($t = 3.25$, $P = 0.00158$), as well as between WT and GagPR67 ($t = 3.73$, $P \leq 0.001$), and the difference in sphericity index between the populations of WT and *amb*438 particles was also significant ($t = 4.65$, $P \leq 0.001$). This suggested that the carboxy terminus of Pr55Gag would play some

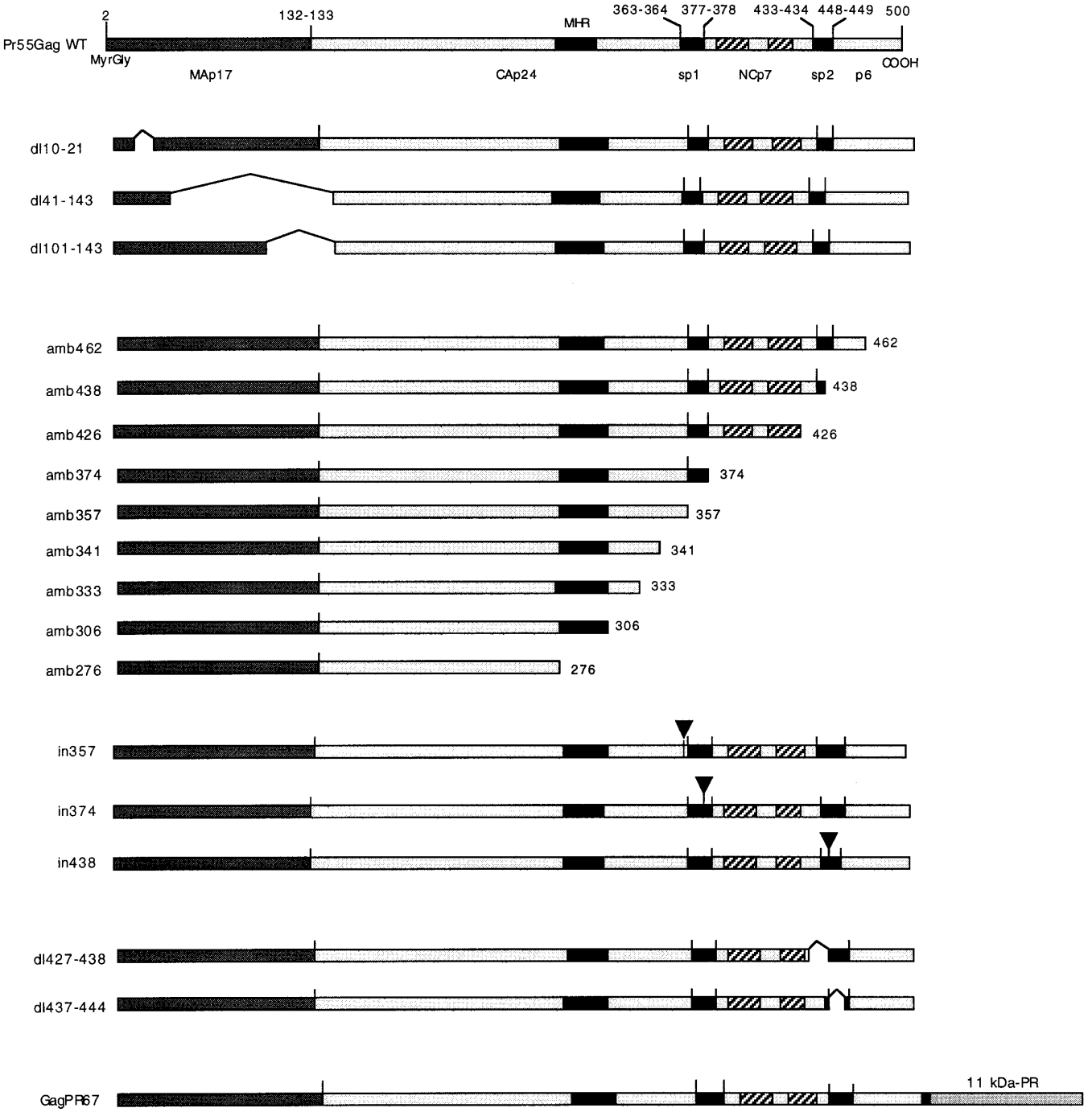

FIG. 1. Schematic diagram of HIV-1_{LAI} Gag contructs depicting the position and the extent of the various truncations and deletions. On the linear representation of the WT Pr55Gag precursor, the respective positions of the structural domains, indicated by vertical bars, are within residues 1–132 (MA), 133–363 (CA), 364–377 (SP1), 378–433 (NC), 434–448 (SP2), and 449–500 (p6). The CA, NC, and p6 domains are shown by light gray boxes, the MA, the major homology region (MHR) of the CA domain, the SP1, and SP2 spacer peptides by black boxes, and the two zinc fingers in the NCp7 by hatched boxes. Gag mutants are arbitrarily grouped according to the type of mutation. From the top to the bottom: MA deletion mutants, carboxy-truncated Gag polyproteins resulting from the insertion of amber multiple stop codons (Carrière *et al.,* 1995), insertion mutants (solid arrows), internal deletion mutants in SP1 or SP2, and polyprotein fusion mutant GagPR67, resulting from the fusion of an inactive protease domain (PR, 11 kDa) to the carboxy-terminal residue of $p6^{gag}$ (Royer *et al.,* 1997).

subtle but significant conformational role in the Gag particle morphogenetic process.

The processing of HIV-1 Pr55Gag by the virus-coded proteinase (PR) results in the release of four major structural domains, MA, CA, NC, and $p6^{gag}$, along with two spacer peptides delineated by additional cleavage sites at the CA–NC junction (position 363–364) and the NC-$p6^{gag}$ junction (position 433–434), respectively (Craven

TABLE 1

Characteristics of Recombinant Gag Precursor Mutants and Mutant Gag Particles[a]

Gag clone designation	Mutant sequence	Domains involved[b]	Sample size[c] (*n*)	Particle morphology	Postulated symmetry[d]
WT Pr55Gag	—	—	51	Spherical	SS
*dl*10-21	$-G^{10}$-[ ]-$L^{21}-$	MA (E^{11}LDRWEKIR^{20})	55	Spherical	SS
*dl*41-143	$-E^{40}$ [NSR] $H^{144}-$	MA, MA//CA[b]	57	Spherical	SS
*dl*101-143	$-A^{100}$ [GINSR] $H^{144}-$	MA//CA	48	Spherical	SS
*amb*276	$-M^{276}$-stop	CA (−HMR)[e]	0	No particle	—
*amb*306	$-A^{306}$-stop	CA (+HMR)[e]	18	Tubular	H
*amb*333	$-I^{333}$[FWNSSLD]-stop	CA	16	Tubular	H
*amb*341	$-A^{341}$[GILV]-stop	CA	30	Tubular	H
*amb*357	$-G^{357}$[WNSSLD]-stop	CA//SP1	21	Tubular	H
*amb*374	$-A^{374}$[GILV]-stop	SP1	24	Spherical	SS
*amb*426	$-C^{426}$[LEF]-stop	NC	24	Spherical	SS
*amb*438	$-W^{438}$[LEF]-stop	SP2	50	Spherical	SS
*amb*462	$-S^{462}$[WNSSLD]-stop	p6*gag*	48	Spherical	SS
*in*357	$-G^{357}$ [WNSS] H −	CA//SP1	10	Spherical and tubular	SS, H
*in*374	$-A^{374}$ [GIPA] T −	SP1	89	Spherical	SS
*in*438	$-W^{438}$ [LEFQ] P −	SP2	16	Spherical	SS
*dl*427-438	$-C^{426}$ [LEFQ] $P^{439}-$	NC//SP2	47	Spherical	SS
*dl*437-444	$-K^{436}$ [L] $P^{445}-$	SP2	62	Spherical	SS
GagPR67	GagPr55-PRD33G[f]	p6*gag*//PR(11kDa)	24	Spherical and tubular	SS, H

[a] The sequences are written in single-letter code amino acids, and amino acids inserted at cloning cassettes are in brackets.

[b] The respective positions of the different structural domains of HIV-1_{LAI} Pr55Gag are indicated in Fig. 1. For the MA mutant *dl*10-21, the short deleted sequence (residues 11–20) is shown in parenthesis. Double slash bars indicate the junction between structural domains.

[c] Sample size represents the number of particles (*n*) observed under the EM and quantitated, as shown in Fig. 2.

[d] Assembly of Gag molecules has been shown not to follow the icosahedral symmetry, but a mechanism of interaction of membrane-bound semispherical sectors (SS) (Fuller *et al.,* 1997). Tubular or filamentous particles are assumed to adhere to helical (H) symmetry.

[e] Deletion involving (−) or not (+) the major homology region (MHR, Wills and Craven, 1991), located within residues 285–305 in HIV-1 Pr55Gag.

[f] Addition of the active site-inactivated protease (PR) domain (D to G substitution; Royer *et al.,* 1997) to the C-terminus of p6*gag*.

and Parent, 1996; Henderson *et al.,* 1992). The role of SP1 (residues 364–377) and SP2 (residues 434–447) in Gag particle morphogenesis was also analyzed by EM, using Pr55Gag carrying mutations in (or near) these two intermediate domains. Mutants *dl*437-444 (SP2-deleted; Fig. 3c), *dl*427-438, carrying a deletion involving the NC-SP2 junction (Fig. 3d), and the SP2 insertion mutant *in*438 showed Gag particles with a mean diameter greater than that of WT particles (145.63, 152.60, and 145.81 nm, respectively), with a significantly higher dispersion of the values (SD ranging from 22 to 36 nm). For the two deletion mutants, but not for the insertion mutant *in*438, there was a lower sphericity index (0.77 and 0.80), compared to WT particles. Two insertion mutants, *in*374, which carried an insertion within the SP1 domain, and *in*357, carrying an insertion at the CA-SP1 junction (Table 1), assembled particles slightly larger than those of the WT (136.94 and 129.84 nm, respectively). However, *in*357 Gag particles appeared to be highly pleiomorphic, with a SD value of 48 nm, and showed many irregular and tubular structures which lowered their sphericity index to 0.77. These data suggested that the spacer domains SP2 and SP1 play a significant role in the Gag particle morphology. The importance of SP1 and the CA–SP1 junction was confirmed by EM analysis of Gag carboxy-truncation mutants.

Carboxy-truncated Gag polyproteins with extensive deletions from the C-terminus were studied in EM for size and shape characteristics. Mutant *amb*276, deleted of p6, SP2, NC, SP1, and the C-terminal third of CA, including the major homology region (MHR; Wills and Craven, 1991; Craven and Parent, 1996), failed to assemble any Gag particle. However, *amb*306, which failed to form spherical particles, assembled long tubular structures of 15 to 93 nm in diameter (60 $\pm$ 27 nm; $m \pm$ SD) and heterogeneous in length, up to 8 μm (Figs. 2a and 4a). Similar tubular assemblies of heterogeneous lengths protruding from the plasma membrane were observed with *amb*333, *amb*341, and *amb*357 (Figs. 4b–4f), although they showed less heterogeneity in diameter (32 $\pm$ 4, 48 $\pm$ 5, and 45 $\pm$ 15 nm, respectively) than *amb*306. These tubular structures were labeled with anti-CA monoclonal antibody and immunogold-labeled conjugate (Fig. 4e), suggesting that the protein layer underneath the membrane lipid bilayer consisted of Gag precursor molecules. All the other Gag mutants carrying smaller carboxy-terminal deletions, *amb*374 (lacking NC, SP2, and p6*gag*; Fig. 4g) *amb*426, *amb*438 (lacking SP2 and p6*gag*), and *amb*462 (deleted of the p6*gag* C-terminal half), assembled spherical particles (not shown; refer to Carrière *et al.,* 1995).

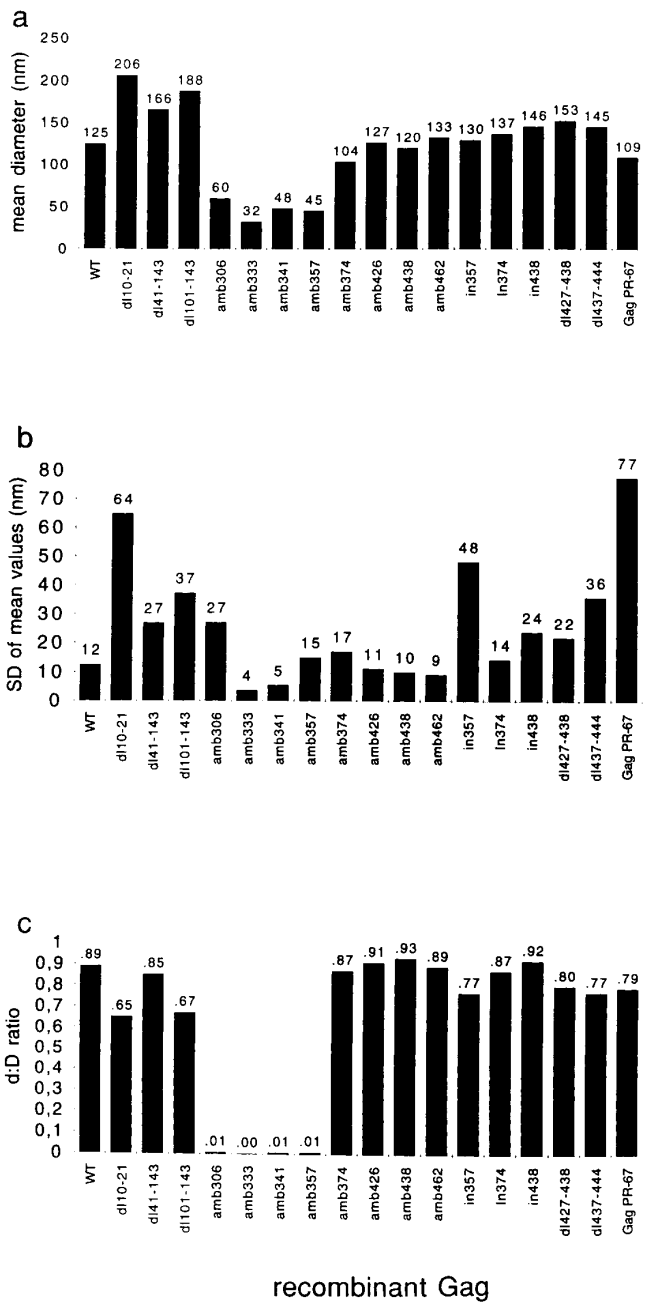

FIG. 2. Histograms of the distribution of Gag particle size (a), heterogeneity (b), and sphericity (c) between different HIV-1 Gag precursor mutants, whose names were abbreviated as indicated in Fig. 1 and Table 1 (a) The mean diameters of the particles are given in nm. For tubular particles of mutants *amb*306, *amb*333, *amb*341, and *amb*357, the parameters shown are the mean diameter taken at different positions (at least 10) of several independent tubes (*n*, refer to Table 1). (b) Particle heterogeneity, evaluated by the standard deviation (SD) to the mean diameters, is given in nm. (c) Particle sphericity was estimated from the ratio of the minimum to maximum diameters; for tubular particles assembled by mutants *amb*306, *amb*333, *amb*341, and *amb*357, this was evaluated by the ratio of the mean diameter to the length of the tube. For *amb*357, the circles and ellipses which resulted from the incidence of the cell sectioning through self-folding tubes, as visible in Fig. 4f, were not quantitated, as they represented too complex 3D structures to be easily interpreted and resolved in a 2D analysis. The sample size, i.e., the number of particles quantitated (*n*), is indicated in Tables 1 and 2.

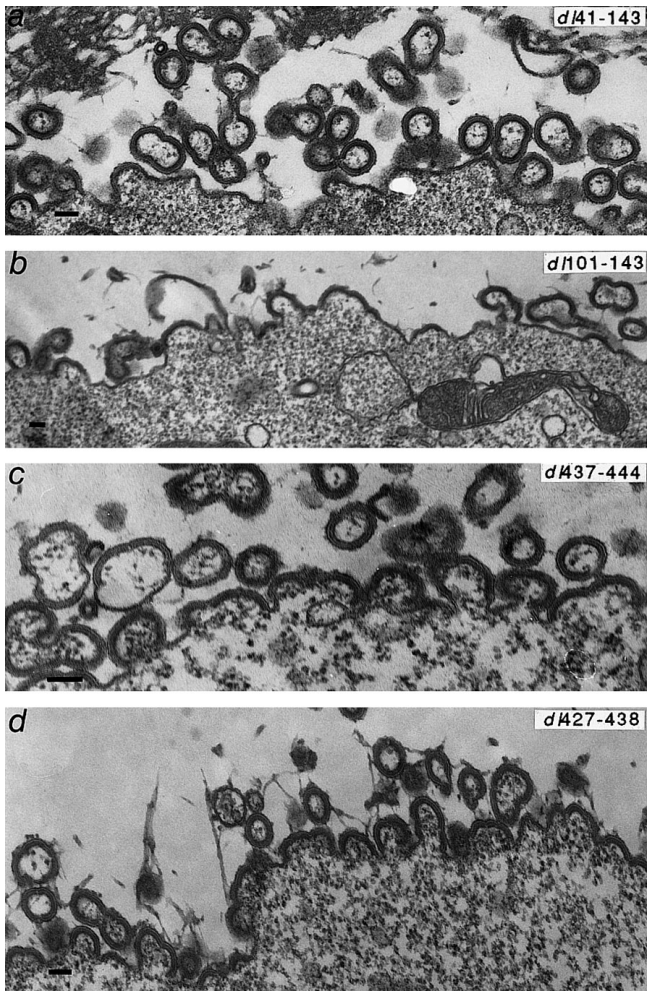

FIG. 3. Electron microscopy of Gag particles of internal deletion mutants, assembling at and budding from Sf9 plasma membrane. MA and MA–CA deletion mutants *dl*41-143 (a) and *dl*101-143 (b); SP2 and NC-SP2 deletion mutants *dl*437-444 (c) and *dl*427-438 (d). Bar, 100 nm.

DISCUSSION

The regions of Pr55Gag which influenced the overall particle size, their variability in size and their degree of sphericity were found to be located at five discrete regions of the molecule: (i) at the N-terminus of the MA, within residues 10–21, (ii) at the MA–CA junction, (iii) at the CA–SP1 junction, (iv) at the NC–SP2 junction, and (v) at the $p6^{gag}$ C-terminus. It is noteworthy that three of these regions correspond to HIV-1 protease cleavage sites, suggesting that they represent accessible and flexible hinges between structural domains. It is reasonable to conceive that these hinges could have significant morphopoietic effects on the Gag particles.

The central portion of the MA domain has been shown to be essential for production of infectious virions and assembly of recombinant Gag particles (Chazal *et al.,* 1995; Freed *et al.,* 1994; Yu *et al.,* 1992). Its two bounding domains, the H1 α-helix, which was mutated in *dl*10-21, and which has been assigned to bind to plasma mem-

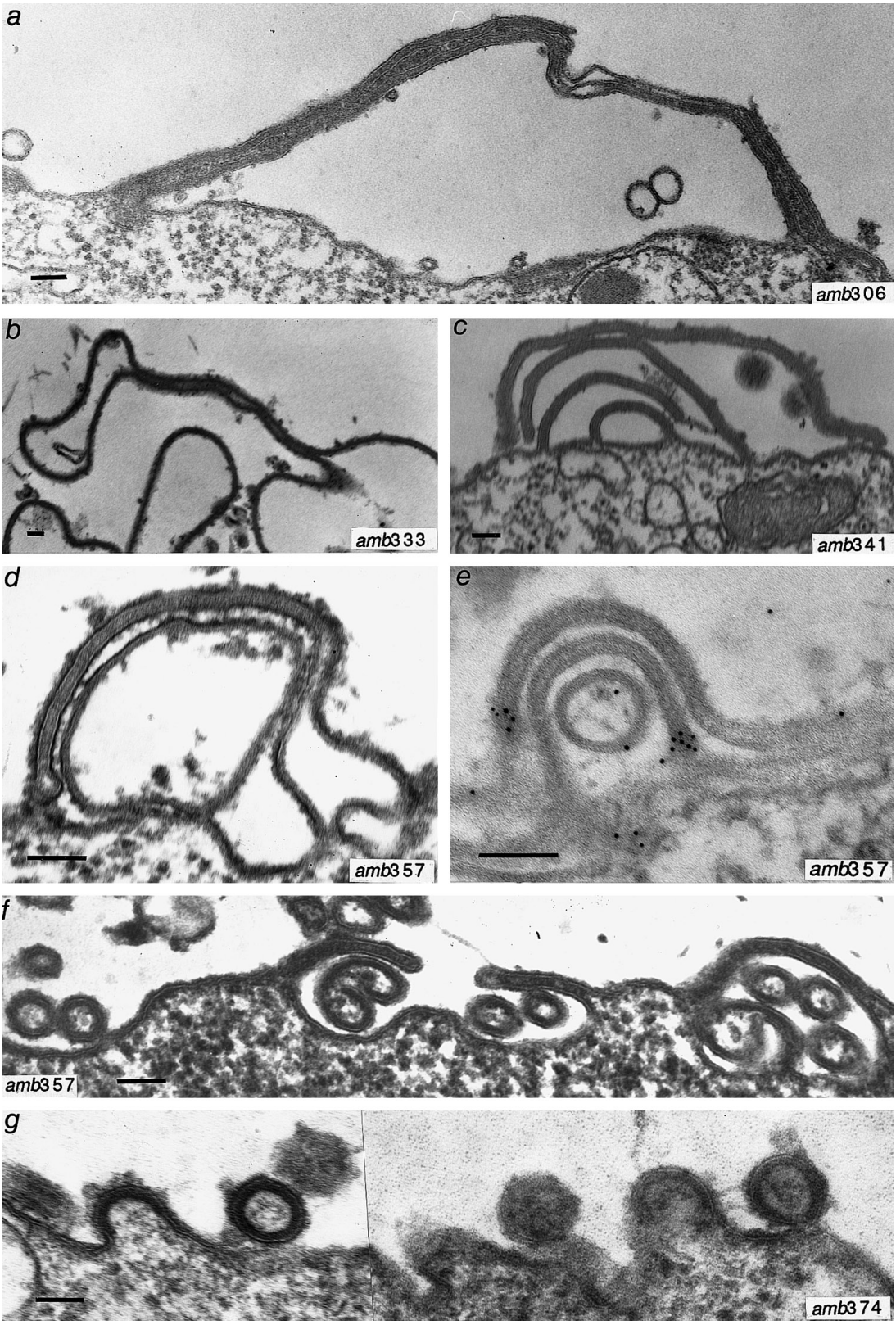

FIG. 4. Electron microscopy (a–d, f, g) and immunoelectron microscopy (e) of Gag particles assembled by Gag carboxy-truncated mutants (amber mutation, *amb*) at the plasma membrane of Sf9 cells. CA deletion mutants *amb*306 (a), *amb*333 (b), *amb*341 (c), *amb*357 (d–f), and *amb*374 (g). In (e), cell section was reacted with anti-CA mAb and 5-nm gold-labeled anti-mouse IgG conjugate. Bar, 100 nm.

TABLE 2

Degree of Sphericity of WT and Mutant Gag Particles[a]

Clone	d:D ratio (mean)	± SD	Sample size (*n*)
WT Pr55Gag	0.89	0.01	51
*dl*10-21	0.65	0.20	55
*dl*41-143	0.85	0.12	57
*dl*101-143	0.67	0.21	48
*amb*306	0.01	NA[b]	18
*amb*333	0.00	NA	16
*amb*341	0.01	NA	30
*amb*357	0.01	NA	21
*amb*374	0.87	0.09	24
*amb*426	0.91	0.08	24
*amb*438	0.93	0.06	50
*amb*462	0.89	0.07	48
*in*357	0.77	0.22	10
*in*374	0.87	0.08	89
*in*438	0.92	0.06	16
*dl*427-438	0.80	0.14	47
*dl*437-444	0.77	0.16	62
GagPR67	0.79	0.20	18

[a] The sphericity index of Gag particles was estimated from the mean ratio of the minimal (*d*) to the maximal (*D*) diameter. The histogram is shown in Fig. 2c. The sample size (*n*) represents the number of particles quantitated. SD, standard deviation of the mean.

[b] NA, not applicable (tubular or filamentous particles).

brane phospholipids (Kräusslich and Welker, 1996), and the C-terminal portion of the MA, overlapping the second basic signal and the MA–CA junction, mutated in *dl*101-143, apparently contain major morphological determinants, influencing the particle size and shape. At the C-terminus of the Gag precursor molecule, partial or total deletion of the $p6^{gag}$ domain resulted in a slight, albeit statistically significant, increase in particle homogeneity and sphericity (as in *amb*462 and *amb*438), whereas the addition of an extra retroviral sequence to the C-terminus of $p6^{gag}$ (as in GagPR67) had the reverse effect. This would imply that the $p6^{gag}$ domain would also have some influence on Gag conformation and assembly, as previously suggested (Hughes *et al.,* 1993; Royer *et al.,* 1997).

Our results with *amb*276 and *amb*306 suggested that a recombinant HIV-1 Gag precursor consisting of the MA and carboxy-truncated CA domains was not capable of self-assembly *in vivo* without the MHR sequence (residues 285–305; Wills and Craven, 1991; Craven and Parent, 1996), confirming previous studies on HIV-1 and other retroviruses (Carrière *et al.,* 1995; Craven *et al.,* 1995; Mammano *et al.,* 1994; Strambio-de-Castilla and Hunter, 1992). The addition of a CA sequence comprising the MHR brought enough assembly information to allow the formation of cylindrical or filamentous Gag particles. These types of structures suggested a helical symmetry of Gag packing. Further extension of the CA domain within residues 307 to 357, as in *amb*333, *amb*341, and *amb*357 which still assembled filamentous particles, implied that the CA sequence within residues 307–357 did not influence the helical symmetry of HIV-1 Gag packing already conferred by the MHR.

The role of Gag spacer peptides in retrovirus particle assembly and infectious virus production has been already investigated in RSV and HIV. The peptide interspacing the CA and NC domains of RSV Gag precursor, although having no significant sequence homology with HIV SP1, has been found to be required for forming regular-shaped infectious virions (Craven *et al.,* 1993; Krishna *et al.,* 1998). Likewise in HIV-1, deletions of SP1 or mutations at the CA–SP1 junction abolished infectivity (Goettlinger *et al.,* 1989; Kraüsslich *et al.,* 1995; Pettit *et al.,* 1994). The integrity of SP1 and the CA–SP1 junction has been found to be crucial for viral particle formation in HIV-1 (Accola *et al.,* 1998), and the deletion of a proline-rich region at the CA–NC junction of recombinant HIV-2 Gag precursor (within residues 372–377) abolished particle assembly (Luo *et al.,* 1994). Viral particles released by COS 7 cells transfected by a SP1-deleted HIV-1 provirus have been found to contain a tube-shaped electron-dense core (Kraüsslich *et al.,* 1995). It has been suggested that SP1 deletion had a deleterious effect on the sequential processing of Gag polyprotein (Pettit *et al.,* 1994) and ordered assembly of the virions (Kraüsslich *et al.,* 1995). Our observation that *amb*357 assembled Gag tubular structures confirmed previous studies using C-truncated mutants of HIV-1 Gag (Gheysen *et al.,* 1989; Goettlinger *et al.,* 1989; Hockley *et al.,* 1994; Jowett *et al.,* 1992) and point mutants of the CA domain of M-PMV Gag precursor (Strambio-de-Castilla and Hunter, 1992). These tubes were also reminiscent of the elongated structures obtained in experiments of *in vitro* assembly of CA–NC domains of RSV and HIV (Campbell and Vogt, 1995) and of HIV-1 recombinant CA protein (Ehrlich *et al.,* 1992; Gross *et al.,* 1997).

Full-length recombinant Gag precursor and immature HIV-1 particles have recently been shown to lack an icosahedral organization, as previously hypothesized (Nermut and Hockley, 1996), and to assemble via accretion of membrane-bound semispherical sectors (Fuller *et al.,* 1997). Furthermore, crystals of RSV CA protein show a helical arrangement of protein subunits (Kovari *et al.,* 1997). The addition to the *amb*357 sequence of a short stretch of amino acids from the CA-SP1 domains, overlapping the CA carboxy-terminal hexapeptide (residues 358–363) and almost the entire SP1 (viz. 11 residues of the SP1 tetradecapeptide), to generate *amb*374, resulted in the assembly of Gag spherical particles (compare panels f and g in Fig. 4). Although smaller than WT Gag particles (103.66 ± 16.98 nm, $n = 24$, confidence interval of 11.4 nm at the $P = 0.05$ level), the *amb*374 particles were almost as homogeneous in size as WT particles and presented a similar sphericity index (0.87; Fig. 2c; Table 2). The modification of the phenotype of Gag particles, from a tubular (as for *amb*306, *amb*333, *amb*341, and *amb*357) to a spherical shape (as for *amb*374), suggested that the addition of the CA–SP1 junc-

tion and SP1 peptide to the MA–CA domains of HIV-1 was sufficient to alter the helical symmetry of assembly of the Gag molecules.

However, recombinant HIV-1 CA protein has been found to self-assemble *in vitro* as tubules, regardless of the presence of SP1 at the C-terminus (Gross *et al.,* 1997). Their diameter, 55 nm, is similar to the value found for our *amb*357 mutant filamentous particles (45 ± 15 nm; Figs. 2a and 2b). This would confirm that the peptide domain conferring the helical symmetry of Gag packing *in vitro* and *in vivo* is localized within the CA, but would imply that the morphopoiteic function assigned to SP1 would take place only *in vivo* at the budding sites, in the presence of the MA domain, and in the plasma membrane environment. Our observation therefore suggests a novel function for the SP1 domain and the CA–SP1 junction of HIV-1, acting as a spherical shape determinant of the immature Gag particle *in vivo* and as a silencer of the helical symmetry of MA–CA assembly, conferred by the MHR and the downstream CA sequence, within residues 307–357. This function and the morphopoietic requirement for the SP1 domain to achieve normal CA assembly would explain the selective advantage of a relatively slow cleavage of the CA–SP1 site by the viral protease compared to the downstream site SP1–NC, as experimentally observed (Pettit *et al.,* 1994).

The minimum sequence required to transform the Gag particle phenotype was the peptide motif ^{358}HKARVLAEAMSQVTNSA^{374}, which differentiates *amb*357 from *amb*374. This peptide was compared to sequences deposited in databanks using the FASTA program. It was found to present 52% homology within a 14-residue overlap and 66% homology within a 9-residue overlap, with the sequence KPRIAEMICDIDN(T) found in the nucleocapsid proteins (residues 238–250) of two paramyxoviruses, human measles virus (MV), and canine distemper virus (CDV) (Barrett and Mahy, 1984; Rozenblatt *et al.,* 1985). The CDV and MV nucleocapsid proteins interact with the M proteins during virion formation and have been postulated to confer the helical symmetry to the nucleoprotein core of the virus. Both Gag CA–SP1 junction (Accola *et al.,* 1998) and MV–CDV nucleoprotein homologous peptide have a high probability of adopting an α-helix conformation within the context of the whole protein (data not shown). It would be rewarding to determine whether the conserved 14-mer peptide motif has any morphopoietic function in a viral protein context different from HIV-1 Gag and represents per se a specific determinant of the symmetry of the CDV and MV cores.

MATERIALS AND METHODS

Gag constructs

The construction of the recombinant baculoviruses expressing the WT Pr55Gag and most of the mutants used in this study has been described in detail elsewhere (Carrière *et al.,* 1995; Chazal *et al.,* 1995; Royer *et al.,* 1991, 1992). Carboxy-truncated mutant *amb*462 has been deleted of the C-terminal half of the p6 domain, *amb*438 of the entire p6 and the C-terminal half of the SP2 intermediate domain, *amb*426 of the p6 and SP2 domains of the C-terminal region of the NC downstream to the second zinc finger, *amb*374 has been deleted of the entire NC, and *amb*357 of SP1 and NC. Further carboxy truncations within the CA domain have generated mutants *amb*341, *amb*333, *amb*306, and *amb*276 (Carrière *et al.,* 1995). The internal deletion in mutant *dl*437-444 (residues ^{437}IWPSYKGR^{444}) removed most of the SP2 domain (^{434}LGKIWPSYKGRPGNF^{448}) (Huvent *et al.,* 1998). Deletion in mutant *dl*427-438 involved the NC-SP2 junction, with the sequence ^{426}CTERQANF–LGKIWP^{439} replaced by ^{426}C-[LEFQ]-P^{439} (Huvent *et al.,* 1998). The MA deletion mutant *dl*10-21 has been characterized in a previous study (Chazal *et al.,* 1995). For MA mutant *dl*41-143, the 5′ *gag* sequence, coding for the MA N-terminal domain, was cut at the *Alu*I site at codon position 40 and ligated to the 3′ moiety of *in*143 *gag,* cut, and blunted at the unique*Eco*RI site present in its insertion linker (Chazal *et al.,* 1994). For mutant *dl*101-143, the *gag* 5′ sequence of the insertion mutant *in*100 was ligated to the 3′ moiety of *in*143 *gag,* both cut and blunted at their unique *Eco*RI site (Chazal *et al.,* 1994). The abbreviated names and sequence characteristics of the mutants used in this study are summarized in Table 1, and a schematic drawing of the Gag precursor domains depicting the position and extent of the various mutations is shown in Fig. 1.

Ultrastructural analysis

Sf9 cells were infected by recombinant baculovirus at a M.O.I. of 5 PFU/cell, and cells expressing the different Gag constructs were harvested at 48 h after infection. To retain the maximum number of budding Gag particles at the periphery of the cells, fibrinogen was added to the cell suspension (5 mg/ml in Tris-buffered saline; TBS), and clotting of fibrin within the cell pellet was induced by addition of thrombin (100 μg/ml in 0.1% $CaCl_2$ in H_2O) immediately before low-speed centrifugation of the cells. Cell pellets were then processed for EM analysis as previously described (Carrière *et al.,* 1995). Several cell sections per each Gag mutant were examined under the Hitachi-H7100 electron microscope. Except for some low Gag particle producers, the parameters were usually determined on 40 to 60 Gag particles per mutant.

For immunoelectron microscopy (IEM), thin sections were pretreated with a saturated aqueous solution of sodium metaperiodate for 10 min, followed by a rinse in H_2O, and 10 min in 0.1 N HCl. After etching, the grids were washed in H_2O for 5 min and incubated on drops of TBS supplemented with 0.05% Tween 20 (TBS-T), 0.5%

cold water fish skin gelatin (Sigma), 0.5% nonimmune goat serum, 0.5% bovine serum albumin, and the required antibody (Bendayan and Zollinger, 1983). Incubation with the primary anti-CA monoclonal antibody (Epiclone 5001; diluted to 1:100) was carried at 4°C overnight (Carrière *et al.,* 1995), followed by reaction with secondary 5-nm colloidal gold-labeled anti-mouse IgG antibody (Amersham; diluted to 1:10) at room temperature for 1 h.

ACKNOWLEDGMENTS

This work was financially supported by the Agence Nationale de Recherche contre le SIDA (ANRS, AC-14 Program). N.C. was the recipient of a postdoctoral fellowship from the ANRS. We thank Saw See Hong for fruitful discussions during the completion of this study, Liliane Cournud for her efficient secretarial aid, and Marthe-Elisabeth Eladari and Jean-Paul Lévy for their constant moral support.

REFERENCES

Accola, M. A., Höglund, S., and Göttlinger, H. G. (1998). A putative α-helical structure which overlaps the capsid-p2 boundary in the human immunodeficiency virus type 1 Gag precursor is crucial for viral particle assembly. *J. Virol.* 72, 2072–2078.

Barrett, T., and Mahy, B. W. J. (1984). Molecular cloning of the nucleoprotein gene of canine distemper virus. *J. Gen. Virol.* 65, 549–557.

Bendayan, M., and Zollinger, M. (1983). Ultrastructural localization of antigenic sites on osmium-fixed tissues applying the protein A-gold technique. *Histochem. Cytochem.* 31, 101–109.

Boulanger, P., and Jones, I. (1996). Use of heterologous expression systems to study retroviral morphogenesis. *In* "Current Topics in Microbiology and Immunology, Retroviral Morphogenesis and Maturation" (H. G. Kräusslich, Ed.), Vol. 214, pp. 237–259. Springer-Verlag, Heidelberg.

Campbell, S. J., and Vogt, V. M. (1995). Self-assembly *in vitro* of purified CA-NC proteins from Rous sarcoma virus and human immunodeficiency virus type 1. *J. Virol.* 69, 6487–6497.

Carrière, C., Gay, B., Chazal, N., Morin, N., and Boulanger, P. (1995). Sequence requirements for encapsidation of deletion mutants and chimeras of human immunodeficiency virus type 1 Gag precursor into retrovirus-like particles. *J. Virol.* 69, 2366–2377.

Chazal, N., Carrière, C., Gay, B., and Boulanger, P. (1994). Phenotypic characterization of insertion mutants of the human immunodeficiency virus type 1 Gag precursor expressed in recombinant baculovirus-infected cells. *J. Virol.* 68, 111–122.

Chazal, N., Gay, B., Carrière, C., Tournier, J., and Boulanger, P. (1995). Human immunodeficiency virus type 1 MA deletion mutants expressed in baculovirus-infected cells: *cis* and *trans* effects on the Gag precursor assembly pathway. *J. Virol.* 69, 365–375.

Craven, R. C., and Parent, L. J. (1996). Dynamic interactions of the Gag polyprotein. *In* "Current Topics in Microbiology and Immunology, Retroviral Morphogenesis and Maturation" (H. G. Kräusslich, Ed.), Vol. 214, pp. 65–94. Springer-Verlag, Heidelberg.

Craven, R. C., Leure-du-Prée, A. E., Erdie, C. R., Wilson, C. B., and Wills, J. W. (1993). Necessity of the spacer peptide between CA and NC in the Rous sarcoma virus Gag protein. *J. Virol.* 67, 6246–6252.

Craven, R. C., Leure-du-Prée, A. E., Weldon, R. A., and Wills, J. W. (1995). Genetic analysis of the major homology region of the Rous sarcoma virus Gag protein. *J. Virol.* 69, 4213–4227.

Ehrlich, L. S., Agresta, B. E., and Carter, C. A. (1992). Assembly of recombinant human immunodeficiency virus type 1 capsid protein *in vitro*. *J. Virol.* 66, 4874–4883.

Freed, E. O., Orenstein, J. M., Buckler-White, A. J., and Martin, M. A. (1994). Single amino acid changes in the human immunodeficiency virus type 1 matrix protein block virus particle production. *J. Virol.* 68, 5311–5320.

Fuller, S. D., Wilk, T., Gowen, B. E., Kräusslich, H.-G., and Vogt, V. M. (1997). Cryoelectron microscopy reveals ordered domains in the immature HIV-1 particle. *Curr. Biol.* 7, 729–738.

Gamble, T. R., Vajdos, F. F., Yoo, S., Worthylake, D. K., Houseweart, M., Sundquist, W. I., and Hill, C. P. (1996). Crystal structure of human cyclophilin A bound to the amino-terminal domain of HIV-1 capsid. *Cell* 87, 1285–1294.

Gamble, T. R., Yoo, S., Vajdos, F. F., von Schwedler, U. K., Worthylake, D. K., Wang, H., McCutcheon, J. P., Sundquist, W. I., and Hill, C. P. (1997). Structure of the carboxyl-terminal dimerization domain of the HIV-1 capsid protein. *Science* 278, 849–853.

Gelderblom, H. (1990). Morphogenesis, maturation and fine structure of lentiviruses. *In* "Retroviral Proteases: Maturation and Morphogenesis" (L. H. Pearl, Ed.), pp. 159–180. Stockton, New York.

Gheysen, D., Jacobs, E., de Foresta, F., Thiriart, C., Francotte, M., Thines, D., and De Wilde, M. (1989). Assembly and release of HIV-1 precursor Pr55*gag* virus-like particles from recombinant baculovirus-infected insect cells. *Cell* 59, 103–112.

Gitti, R. K., Lee, B. M., Walker, J., Summers, M. F., Yoo, S., and Sundquist, W. I. (1996). Structure of the amino-terminal core domain of the HIV-1 capsid protein. *Science* 273, 231–235.

Göttlinger, H. G., Sodrosky, J. G., and Haseltine, W. A. (1989). Role of capsid precursor processing and myristoylation in morphogenesis and infectivity of human immunodeficiency virus type 1. *Proc. Natl. Acad. Sci. USA* 86, 5781–5785.

Gross, I., Hohenberg, H., and Kräusslich, H.-G. (1997). *In vitro* assembly properties of purified bacterially expressed capsid proteins of human immunodeficiency virus. *Eur. J. Biochem.* 249, 592–600.

Henderson, L. E., Bowers, M. A., Sowder, R. C. II, Serabyn, S. A., Johnson, D. G., Bess, J. W., Arthur, L. O., Bryant, D. K., and Fenselau, C. (1992). Gag proteins of the highly replicative MN strain of human immunodeficiency virus type 1: Posttranslational modifications, proteolytic processing, and complete amino acid sequences. *J. Virol.* 66, 1856–1865.

Hill, C. P., Worthylake, D. K., Bancroft, D. P., Christensen, A. M., and Sundquist, W. I. (1996). Crystal structure of the trimeric human immunodeficiency virus type 1 matrix protein: Implications for membrane association and domain assembly. *Proc. Natl. Acad. Sci. USA* 93, 3099–3104.

Hockley, D. J., Nermut, M. V., Grief, C., Jowett, J. B. M., and Jones, I. M. (1994). Comparative morphology of Gag protein structures produced by mutants of the *gag* gene of human immunodeficiency virus type 1. *J. Gen. Virol.* 75, 2985–2997.

Hughes, B., Booth, T. F., Belyaev, A. S., McIlroy, D., Jowett, J., and Roy, P. (1993). Morphogenic capabilities of human immunodeficiency virus type 1 *gag* and *gag-pol* proteins in insect cells. *Virology* 193, 242–255.

Huvent, I., Hong, S. S., Fournier, C., Gay, B., Tournier, J., Carrière, C., Vigne, R., Spire, B., and Boulanger, P. (1998). Interaction and coencapsidation of human immunodeficiency virus type 1 Vif and Gag recombinant proteins. *J. Gen. Virol.* 79, 1069–1081.

Jowett, J. B. M., Hockley, D. J., Nermut, M. V., and Jones, I. M. (1992). Distinct signals in human immunodeficiency virus type 1 Pr55 necessary for RNA binding and particle formation. *J. Gen. Virol.* 73, 3079–3086.

Kovari, L. C., Momany, C. A., Miyagi, F., Lee, S., Campbell, S., Vuong, B., Vogt, V. M., and Rossmann, M. G. (1997). Crystals of Rous sarcoma virus capsid protein show a helical arrangement of protein subunits. *Virology* 238, 79–84.

Kräusslich, H.-G., Fäcke, M., Heuser, A. M., Konvalinka, J., and Zentgraf, H. (1995). The spacer peptide between human immunodeficiency virus capsid and nucleocapsid proteins is essential for ordered assembly and viral infectivity. *J. Virol.* 69, 3407–3419.

Kräusslich, H.-G., and Welker, R. (1996). Intracellular transport of retroviral capsid components. *In* "Current Topics in Microbiology and

Immunology, Retroviral Morphogenesis and Maturation" (H. G. Kräusslich, Ed.), Vol. 214, pp. 25–63. Springer-Verlag, Heidelberg.

Krishna, N. K., Campbell, S., Vogt, V. M., and Wills, J. W. (1998). Genetic determinants of Rous sarcoma virus particle size. *J. Virol.* 72, 564–577.

Luo, L., Li, Y., Dales, S., and Kang, C. Y. (1994). Mapping of functional domains for HIV-2 *gag* assembly into virus-like particles. *Virology* 205, 496–502.

Mammano, F., Öhagen, A., Höglund, S., and Göttlinger, H. G. (1994). Role of the major homology region of human immunodeficiency virus type 1 in virion morphogenesis. *J. Virol.* 68, 4927–4936.

Massiah, M. A., Starich, M. R., Paschal, C., Summers, M. F., Christensen, A. M., and Sundquist, W. I. (1994). Three-dimensional structure of the human immunodeficiency virus type 1 matrix protein. *J. Mol. Biol.* 244, 198–223.

Momany, C., Kovari, L. C., Prongay, A. J., Keller, W., Gitti, R. K., Lee, B. M., Gorbalenya, A. E., Tong, L., McClure, J., Ehrlich, L. S., Summers, M. F., Carter, C., and Rossmann, M. G. (1996). Crystal structure of dimeric HIV-1 capsid protein. *Nature Struct. Biol.* 3, 763–770.

Nermut, M., and Hockley, D. J. (1996). Comparative morphology and structural classification of retroviruses. *In* "Current Topics in Microbiology and Immunology, Retroviral Morphogenesis and Maturation" (H. G. Kräusslich, Ed.), Vol. 214, pp. 1–24. Springer-Verlag, Heidelberg.

Overton, H. A., Fuji, Y., Price, I. R., and Jones, I. M. (1989). The protease and *gag* gene products of the human immunodeficiency virus: Authentic cleavage and post-translational modification in an insect cell expression system. *Virology* 170, 107–116.

Pettit, S., Moody, M. D., Wehbie, R. S., Kaplan, A. H., Nantermet, P. V., Klein, C. A., and Swanstrom, R. (1994). The p2 domain of human immunodeficiency virus type 1 Gag regulates sequential proteolytic processing, and is required to produce fully infectious virions. *J. Virol.* 68, 8017–8027.

Rao, Z., Belyaev, A. S., Fry, E., Jones, I. M., and Stuart, D. I. (1995). Crystal structure of of the SIV matrix antigen and implications for virus assembly. *Nature* 378, 743–747.

Royer, M., Cerutti, M., Gay, B., Hong, S. S., Devauchelle, G., and Boulanger, P. (1991). Functional domains of HIV-1 *gag*-polyprotein expressed in baculovirus-infected cells. *Virology* 184, 417–422.

Royer, M., Hong, S. S., Gay, B., Cerutti, M., and Boulanger, P. (1992). Expression and extracellular release of human immunodeficiency virus type 1 Gag precursors by recombinant baculovirus-infected cells. *J. Virol.* 66, 3230–3235.

Royer, M., Bardy, M., Gay, B., Tournier, J., and Boulanger, P. (1997). Proteolytic activity *in vivo* and encapsidation of recombinant human immunodeficiency virus type 1 proteinase expressed in baculovirus-infected cells. *J. Gen. Virol.* 78, 131–142.

Rozenblatt, S., Eizenberg, O., Ben-Levy, R., Lavie, V., and Bellini, W. J. (1985). Sequence homology within the morbilliviruses. *J. Virol.* 53, 684–690.

Strambio-de-Castilla, C., and Hunter, E. (1992). Mutational analysis of the major homology region of Mason-Pfizer monkey virus by use of saturation mutagenesis. *J. Virol.* 66, 7021–7032.

Wills, J. W., and Craven, R. C. (1991). Form, function and use of retroviral Gag proteins. *AIDS* 5, 639–654.

Yu, X. F., Yuan, X., Matsuda, Z., Lee, T. H., and Essex, M. (1992). The matrix protein of human immunodeficiency virus type 1 is required for incorporation of viral envelope protein into mature virions. *J. Virol.* 66, 4966–4971